Available online at www.sciencedirect.com
ScienceDirect
Chinese Journal of Natural Medicines 2021, **19**(10): 741-749
doi: 10.1016/S1875-5364(21)60107-3
Chinese Journal of Natural Medicines

•Reaearch article•

Therapeutic effect of neohesperidin on TNF-α-stimulated human rheumatoid arthritis fibroblast-like synoviocytes

WANG Xiao-He[1, 2Δ], DAI Ce[2Δ], WANG Jun[2], LIU Rui[2], LI Lei[2], YIN Zong-Sheng[2*]

[1] *Department of Bone and Joint Surgery, Institute of Orthopedic Diseases, the First Affiliated Hospital, Jinan University, Guangzhou 510000, China;*
[2] *Department of Orthopedics, the First Affiliated Hospital of Anhui Medical University, Hefei 230000 , China*

Available online 20 Oct., 2021

[ABSTRACT] During the pathogensis of rheumatoid arthritis (RA), activated RA fibroblast-like synoviocytes (RA-FLSs) combines similar proliferative features as tumor and inflammatory features as osteoarthritis, which eventually leads to joint erosion. Therefore, it is imperative to research and develop new compounds, which can effectively inhibit abnormal activation of RA-FLSs and retard RA progression. Neohesperidin (Neo) is a major active component of flavonoid compounds with anti-inflammation and anti-oxidant properties. In this study, the anti-inflammation, anti-migration, anti-invasion, anti-oxidant and apoptosis-induced effects of Neo on RA-FLSs were explored to investigate the underlying mechanism. The results suggested that Neo decreased the levels of interleukin IL-1β, IL-6, IL-8, TNF-α, MMP-3, MMP-9 and MMP-13 in FLSs. Moreover, Neo blocked the activation of the MAPK signaling pathway. Furthermore, treatment with Neo induced the apoptosis of FLSs, and inhibited the migration of FLSs. It was also found that Neo reduced the accumulation of reactive oxygen species (ROS) induced by TNF-α. Taken together, our results highlighted that Neo may act as a potential and promising therapeutic drug for the management of RA.

[KEY WORDS] Neohesperidin; Rheumatoid-arthritis; Fibroblast-like synoviocytes; Inflammatory; Oxidative stress; MAPK
[CLC Number] R965 **[Document code]** A **[Article ID]** 2095-6975(2021)10-0741-09

INTRODUCTION

Rheumatoid arthritis (RA) is an inflammatory and autoimmune disease characterized by synovial hyperplasia and joint destruction, which is a leading cause of high malformation and disability in patients [1]. The typical inflammatory site of RA is activated fibroblast-like synoviocytes (FLSs), which show increased proliferation, prolonged survival, and inflammatory effects. RA-FLSs are the manifestation of synovitis, which may result in joint destruction with cartilage and bone loss due to lack of timely and effective treatment [2]. The mitogen-activated protein kinase (MAPK) signaling pathway including p38, extracellular signal-regulated kinase (ERK), and Jun N-terminal kinase (JNK), is widespread in various organisms, which serves a critical role in gene expression regulation process. This signaling cascade has attracted increasing interest due to its association with multiple pathophysiological processes, such as proliferation, inflammatory, apoptosis and oxidative stress [3]. Furthermore, MAPK activation is considered to participate in the pathsogenesis of RA [4, 5]. With respect to the role of the MAPK signaling pathway in regulating RA, MAPK has been regarded as a potential drug target in the treatment of RA. However, most of MAPK inhibitors still fail in phase III RA trials because of their toxicity or poor efficacy [6].

Neohesperidin (Neo, hesperetin 7-*O*-neohesperidoside, Fig. 1A) is a flavone compound isolated from various dietary sources, such as olive leaves [7] and citrus fruits [8], while it can also be extracted from certain medicinal herbs [9, 10]. Neo exerts anti-inflammatory [11, 12], anti-oxidant [13], anti-proliferative [14], apoptosis-promoting [15], and anti-bacterial effects [16], and can inhibit intracellular ROS accumulation in many diseases [17]. An interesting approach using flavone compound as a MAPK regulator as described by an *in vitro* study showed that polyphenols can significantly affect the MAPK pathway [18]. Neo can induce apoptosis in human pancreatic cells [15]. In addition, Neo has been reported to protect against liver injury in mice and cancers like colorectal tumorigenesis and breast adenocarcinoma [19-21]. With respect to

[Received on] 19-Feb.-2021
[Research funding] This work was supported by the National Natural Science Foundation of China (No. 81672161).
[*Corresponding author] E-mail: anhuiyzs@126.com
[Δ]These authors contributed equally to this work.
These authors have no conflict of interest to declare.

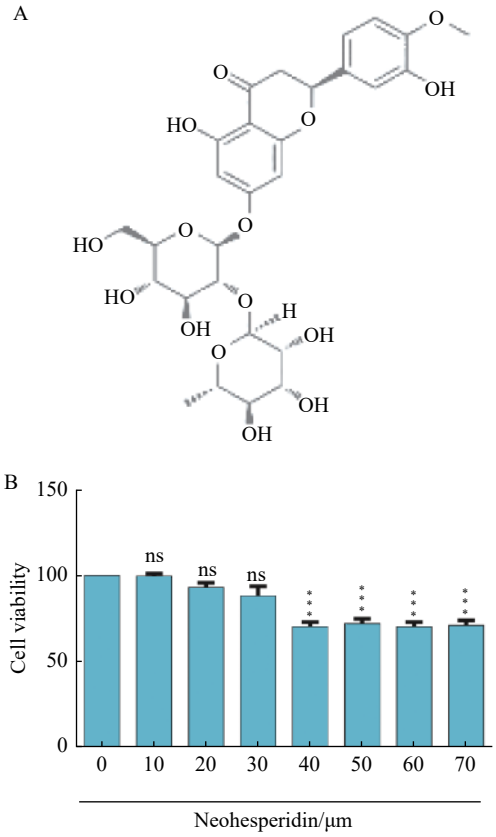

Fig. 1 Chemical structure and the effect of Neo on RA-FLS viability. (A) Chemical structure of Neo. (B) RA-FLSs in 96-well plates were treated with different concentrations of Neo (0.0, 10.0, 20.0, 30.0, 40.0, 50.0, 60.0 and 70.0 μmol·L^{-1}) for 24 h. The medium was removed and cell viability was analyzed by CCK-8 assay. All data are expressed as mean ± SD (n = 3). Statistical difference is represented by $^{***}P < 0.001$, $^{**}P < 0.01$, $^{*}P < 0.05$ *vs* blank group

the characteristics of RA as a typical chronic inflammatory autoimmune disease, Neo may act as a potential natural product and exert anti-inflammatory and chemopreventive effects against RA. However, little information is available concerning the protective effect of Neo against RA. Therefore, in this study, the role of Neo in the treatment of RA was investigated and the underlying molecular mechanisms, especially migration, invasion and proinflammatory cytokines involved were explored.

Materials and Methods

Chemicals and reagents

DMEM medium was purchased from Hyclone (Logan City, Utah, USA). RNA reverse transcription and polymerase chain reaction system was from TaKaRa (TaKaRa Bio, Japan). Goat anti-rabbit IgG and goat anti-mouse IgG were purchased from Wuhan Sanying Biology Technology Co., Ltd. (Wuhan, China). Recombinant human TNF-α was purchased from R&D (Minneapolis, MN, USA). The cell counting kit-8, DCFH-DA ROS detection kit, trypsin, cell lysis solution (RIPA) and penicillin-streptomycin were supplied by Beyotime (Shanghai, China). Collagenase II was obtained from Sigma (St. Louis, USA). Fetal bovine serum was purchased from CLARK (Virginia, USA). ELISA kit was bought from Dakewe Biotech Co., Ltd. (Shenzhen, China). TRIzol reagent was obtained from Invitrogen (CA, USA). Neo, and indometacin (purity > 98%) were bought from MCE China (Shanghai, China). Anti-cleaved caspase-3, Bax, Bcl-2, p38, phosphorylated p38, JNK, phosphorylated JNK, ERK, phosphorylated-ERK antibodies were obtained from Cell Signaling Technology (Boston, USA). Anti-MMP3, MMP9 and MM13 antibodies were purchased from Wuhan Sanying Biology Technology Co., Ltd. (Wuhan, China). Matrigel basement membrane matrix was purchased from BD Biosciences (Oxford, UK). Annexin V-FITC apoptosis kit was purchased from Santa CruzJ. Biotechnology, Inc. (TX, USA). Transwell chamber was bought from Biosciences (CA, USA).

Human primary FLS extraction and culture

Human synovium tissues were obtained from RA patients. All the patients were diagnosed according to the American College of Rheumatology (ACR) 1987 classification criteria for rheumatoid arthritis [22]. The fat, muscle and ligament tissues were removed on an aseptic operation platform, and washed with PBS (including penicillin-streptomycin) for several times, to wipe away blood and fat particles as much as possible. Then, the synovium tissue sample was cut into 1 mm × 1 mm × 1 mm pieces with sterilized scissors and evenly pasted in a 25 cm^2 culture bottle. Then, the culture bottle was slowly erected, to which about 3 mL of high glucose medium containing 10% FBS was slowly added. Then the bottle was vertically placed into an incubator at 37 °C in an atmosphere of 5% CO_2. After about 3−6 h, the culture bottle was placed in a horizontal manner, so that the tissues were submerged within the culture medium. Finally, the culture bottle was placed into the incubator for further cultivation. All the procedures were complied with the rules enacted by the Medical Ethics Committee of Anhui Medical University (reference No.: Quick-PJ-2020-06-19) and followed the guidelines of the Declaration of Helsinki and the International Ethical Guidelines for Biomedical Research Involving Human Subjects.

Cell viability assay

First, the toxicity of Neo on RA-FLS viability was evaluated. The cell viability was determined by cell counting kit-8 (CCK-8) assay. RA-FLSs (1 × 10^4 cells/well) were seeded into 96-well plates and treated with Neo at various concentrations (0.0, 10.0, 20.0, 30.0, 40.0, 50.0, 60.0 and 70.0 μmol·L^{-1}) for 48 h. Then, CCK-8 (10 μL) was added to each well of the plate, and their optical density values at 450 nm were determined by a microplate reader. The cell viability was calculated using the following equation: Cell viability = [OD $_{(Neohesperidin)}$ − OD $_{(blank)}$] / [OD $_{(control)}$ − OD $_{(blank)}$].

Western blot

RA-FLSs were lysed with a mixture of RIPA buffer and PMSF (100 : 1), and protein concentrations were measured using a BCA kit after total protein was purified by high-speed

cryogenic centrifugation (12 000 g·min^{-1}, 10 min, 4 °C). The supernatants mixed with 5 × SDS-PAGE Sample Loading Buffer were separated on 10% SDS-PAGE gel, and then electrophoretically transferred to PVDF membrane (GE Healthcare). The membrane was blocked in TBST-5% nonfat milk at room temperature for 1 h and then incubated at 4 °C overnight with primary antibodies (MMP-3, MMP-9, MMP-13, p38, P-p38, JNK, P-JNK, ERK, P-ERK, Bcl-2, Bax and cleaved-caspase3), followed by incubation with TBST-5% nonfat milk containing goat anti-rabbit IgG or goat anti-mouse IgG at room temperature for 2 h. The membrane was washed with TBST solution before detection of chemiluminescence using BeyoECL Plus.

RT-qPCR

Total cellular RNA containing mRNA was extracted from RA-FLSs by TRIzol Reagent following the manufacturer's instructions. Then, cDNA was synthesized from equal amounts of RNA using 5 × HiScript II qRT SuperMix II in a PTC-100 Programmable Thermal Controller. Gene expression was measured by RT-qPCR on an Agilent Mx3000p. The amplification program was listed as follows: predenaturation at 95 °C for 30 min, then 40 cycles of 95 °C for 5 s and 60 °C for 30 s. Relative gene expression was analyzed by the $2^{-\Delta\Delta Ct}$ method. Primer sequences are shown in Table 1. Indomethacin was used as a positive control, and the levels of MMP9, MMP13, IL-1β, IL-6, IL-8, and TNF-α mRNA were detected.

Table 1 Primer pairs for RT-PCR

Gene	Primers sequences
IL-1β	Forward: 5′-GGACAAGCTGAGGAAGATGC-3′
	Reverse: 5′-TCGTTATCCCATGTGTCGAA-3′
IL-6	Forward: 5′-GAAAGCAAAGAGGCACT-3′
	Reverse: 5′-TTTCACCAGGCAAGTCTCCT-3′
IL-8	Forward: 5′-GGCTTGCTAGGGGAAATGA-3′
	Reverse:5′-AGCTGACTCTGACTAGGAAACTT-3′
MMP-9	Forward: 5′-GCACGACGTCTTCCAGTACC-3′
	Reverse: 5′-GGTTCAACTCACTCCGGGAA-3′
MMP-13	Forward: 5′-GACTTCCCAGGAATTGGTGA-3′
	Reverse: 5′-TGACGCGAACAATACGGTTA-3′
TNF - α	Forward:5′-AGACCTTAGACTGGAGAGATGA-3′
	Reverse:5′-CAAAGACACCTGGCTGGCTGTAAC-3′
OPG	Forward: 5′-CTGCTTATAACTGGAAATGGCC-3′
	Reverse: 5′-CTGTGGCAAAATTAGTCACTGG-3′
RANKL	Forward: 5′-CCCACAATGTGTTGCAGTTC-3′
	Reverse: 5′-TCCTGAGACTCCATGAAAACG-3′
GAPDH	Forward: 5′-ACCCAGAAGACTGTGGATGG-3′
	Reverse: 5′-TTCAGCTCAGGGATGACCTT-3′

Measurement of cytokines by Enzyme-linked Immunosorbent Assay (ELISA)

The levels of TNF-α, IL-1β, IL-6 and IL-8 in the supernatants were measured by human enzyme-linked immunosorbent assay (ELISA) kits according to the manufacturer's instructions. The absorbance of each well was read at 450 nm using a microplate reader. All the experiments were performed in triplicate.

Measurement of cell invasion by transwell

Cell invasive ability was assessed by transwell chamber. Cells were trypsinized and re-suspended with serum-free DMEM medium at a final concentration of 5 × 10^4/mL. Then, 200 μL cell suspension was added into the upper chamber of the Transwell Insert which was coated with Matrigel basement membrane matrix, while 500 μL DMED with 10% FBS was placed in the lower wells as a chemoattractant. After 12-24 h of incubation at 37 °C in an atmosphere of 5% CO_2 , the non-migrating cells on the upper surface of the chamber were removed using a cotton swab. The cells adhering beneath the chamber, which went through the Matrigel basement membrane matrix, were fixed with methanol for 15 min and stained with 0.1% crystal violet for 15 min. The filter was carefully removed with a knife and fixed on a glass slide with resin. The cells were quantified by counting the stained cells that were migrated to the lower side of the filter under an optical microscope. The stained cells were counted as the mean number of cells per six random fields under a contrast microscope.

Measurement of cell migration by wound healing assay

RA-FLSs were placed into a 6-well culture plate and grown to more than 90% confluence. The cells were scratched using a 100 μL sterile pipette tip and washed with PBS twice. DEME medium containing 10% FBS was added to each well with different concentrations of Neo. After 24 h and 36 h, the images for wound areas were captured at random fields using an inverted fluorescence microscope (Olympus, Tokyo, Japan) in three separate experiments. ImageJ2.43s was used to calculate the mobility ratio, and the mobility ratio was presented as the percentage by which the original scratch area decreased at each indicated time point.

Annexin V assay

Cell apoptosis was assessed by the Annexin V-FITC Apoptosis Kit according to the manufacturer's protocol. Cells were seeded in 6-well plates at a density of 5 × 10^5 cells/well overnight. Briefly, the cells were pretreated with 5, 10, 15 or 30 μmol·L^{-1} Neo for 24 h and washed with PBS, before incubation with 5 μL Annexin V-FITC and 5 μL PI in the darkness at room temperature for 20 min. Then, the apoptotic rate was analyzed at 488 nm (excitation) and 525 nm (emission) by a FACSCalibur flow cytometer (Becton & Dickson, San Jose, California).

Intracellular ROS detection

The amounts of reactive oxygen species (ROS) in RA-FLSs were measured by the ROS kit. Cells were seeded at a density of 5 × 10^{5}cell/well in 6 - well plates and cultured

overnight, before exposure to various concentrations of Neo for 24 h. DCFH-DA was diluted to 10 μmol·L^{-1} and added 1 mL in each well. Subsequently, the cells were incubated in the darkness at 37 °C for 30 min and washed with PBS for three times. Then, the representative bright-field and DCFH-DA fluorescence photomicrographs were immediately analyzed under an inverted fluorescence microscope (Olympus, Tokyo, Japan).

Statistical analysis

Statistical analysis was performed following the procedures of GraphPad Prism 5.0. All data are expressed as mean ± SD. The one-way analysis of variance (ANOVA) SPSS V.23.0 (SPSS Inc., Chicago, USA) was used to analyze the differences between groups. $P < 0.05$ was considered to be statistically significant.

Results

Effects of Neo on RA-FLS viability

RA-FLSs were treated with Neo at the concentrations of 0.0, 10.0, 20.0, 30.0, 40.0, 50.0, 60.0 and 70.0 μmol·L^{-1} for 48 h. As shown in Fig. 1 B, the results of the CCK-8 assay indicated that 10, 20, and 30 μmol·L^{-1} Neo resulted in 98%, 92% and 86% cell viability, respectively. However, the viability less than 80% was documented at much higher concentrations of Neo (> 30 μmol·L^{-1}), which was remarkalby differet from the control at 30 μmol·L^{-1} and above ($P < 0.05$). With respect to the lower viability of RA-FLSs, the concentrations of 5–30 μmol·L^{-1} of Neo were used in the following studies concening its effects on RA-FLSs.

Suppression of Neo on the inflammation of RA

As illustrated in Figs. 2A, B, dramatic increases in the amouts of MMP3, MMP9 and MMP13 were detected in the TNF-*α*-stimulated group. Nevertheless, such changes were reduced by pretreatment with Neo in a dose-dependent manner. According to ELISA and qRT-PCR analyses, the levels of pro-inflammatory cytokines, including IL-1*β*, IL-6, IL-8, and TNF-*α* decreased by Neo treatment in a concentration-dependent manner (Figs. 2C−N). Furthermore, qRT-PCR results indicated that Neo up-regulated the expression of OPG mRNA and down-regulated RANKL expression in RA-FLSs (Figs. 2I, J). These findings demonstrated the inhibitory effect of Neo on the inflammation of RA.

Neo inhibits the migration and invasion of primary RA-FLS

RA is characterised by the invasion and migration of RA-FLSs [23]. As shown in Figs. 3A, B, compared with the untreated group, the number of cells that passed through the Matrigel (blue-purple spots) decreased as the drug concentration increased. To further investigate the effect of Neo on the migration of RA-FLSs, the wound healing assay was performed. Then, 24 h after scratching, RA-FLSs started to migrate into the blank area. It was noticeable that the cells treated with 5, 10, or 30 μmol·L^{-1} Neo migrated less than the control cells (26.0%, 16.2% and 9.2% *vs* 36.9%), and the difference became more evident after 36 h (41.0%, 29.2% and 18.2% *vs* 52.9%). Fig. 3 shows that at both 24 h and 36 h (Figs. 3C, D), RA-FLS migration was significantly suppressed by Neo in a concentration- and time-dependent manner. The relative migration was calculated accroding to the ratio of the migrated cells, and the wound healing assay was conducted in triplicate.

Neo alleviates ROS production in RA-FLSs

ROS, an essential and direct source of oxidative injury, is often used as an indicator of oxidative stress. As shown in Figs. 4A, B, after exposure to TNF-*α*, the intensity of green fluorescence was stronger than that in the blank group. However, this change was remarkably reversed after the treatment of Neo. The intensity of intracellular ROS decreased in a concentration-dependent manner. These results indicated that Neo prevents RA-FLSs from intracellular ROS generation.

Effects of Neo on RA-FLS apoptosis

Flow cytometry was used to investigate the function of Neo on cell apoptosis. As shown in Figs. 4C, D, the apoptosis rate of RA-FLSs increased after treatment with Neo. Moreover, with an increased concentration of Neo, the percentage of apoptotic cells was continuously elevated. Western blot was used to measure the levels of Bcl-2, Bax and cleaved-caspase3. As shown in Figs. 5E, F, treatment with Neo substantially down-regulated the expression of Bcl-2, while up-regulating the expression of Bax and cleaved-caspase 3 in a dose-dependent manner, with a decreased ratio of Bcl-2/Bax. These results revealed that Neo can promote RA-FLS apoptosis, contributing to inhibition of RA-FLS growth.

Neo suppresses the activation of MAPK pathway induced by TNF-α in RA-FLSs

Mitogen-activated protein kinase (MAPK), which plays a major role in intracellular oxidative stress response and is embedded in a highly active signaling cascade in RA-FLSs [5], is involved in the pathophysiological process of proliferation, differentiation, apoptosis and invasion [3]. Since Neo inhibited the expression of MMP-3, MMP-9, MMP-13, IL-6, IL-1*β* and TNF-*α* in RA-FLSs and suppressed the viability and invasion of RA-FLSs, it is necessary to investigate the invovlement of the MAPK signaling pathway in these cells. As depicted in Fig. 5, administration of TNF-*α* remarkably activated the phosphorylation levels of p38, ERK and JNK, while treatment with Neo resulted in significant down-regulation in the expression of the above indicators compared with the blank group and TNF-*α*-treated group, in a concentration-dependent manner. These data suggested that Neo exerts its function on RA-FLSs at least partly through suppressing the MAPK signaling pathway.

Discussion

RA-FLS is a special step during the pathologenesis of RA, where persistent inflammatory reactions occur. It can also lead to cartilage degradation and bone destruction due to the tumor-like properties of synovial hyperplasia. However, the application of RA-FLS-targeting drugs like DMARD has been limited to clinical practice in light of its high cost and adverse reactions like toxicity *in vivo*. The development of effective medicine on RA remains an ongoing challenge. In the

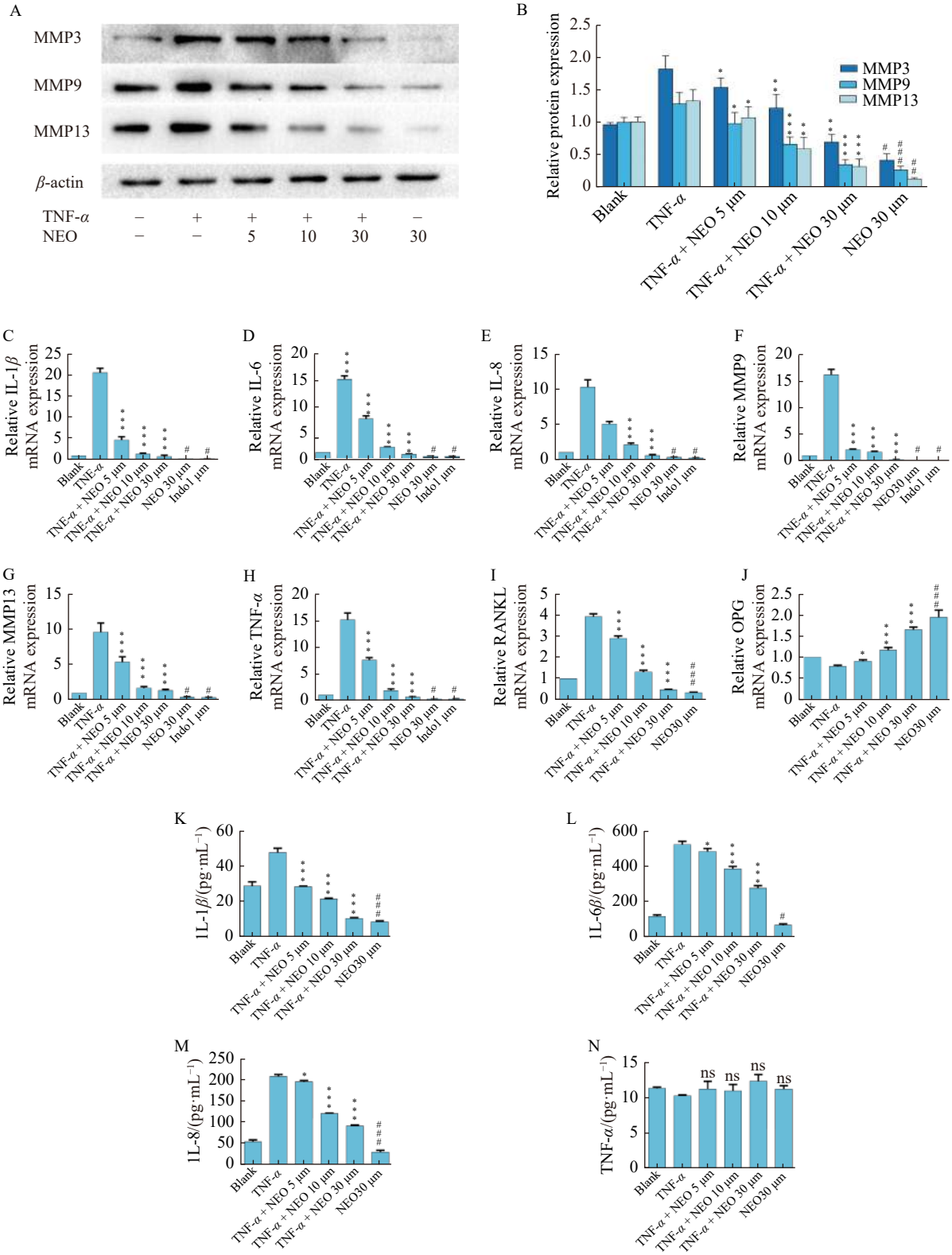

Fig. 2 Effect of Neo on the expression of inflammatory factors in RA-FLSs. (A−B) The amounts of MMP3, MMP9 and MMP-13 in RA-FLSs were measured by Western blot. (C−J) The gene expression of MM9, MMP13, IL-1*β*, IL-6, IL-8, TNF-*α*, RANKL, and OPG in RA-FLSs was detected by RT-qPCR. (K−N) The levels of IL-1*β*, IL-6, IL-8 and TNF-*α* in the supernatant of RA-FLSs were measured by ELISA. All data are expressed as mean ± SD ($n = 3$). Statistical difference is represented by $^{***}P < 0.001$, $^{**}P < 0.01$, $^{*}P < 0.05$ *vs* TNF-*α* sitimulated group. $^{###}P < 0.001$, $^{##}P < 0.01$, $^{#}P < 0.05$ *vs* blank group

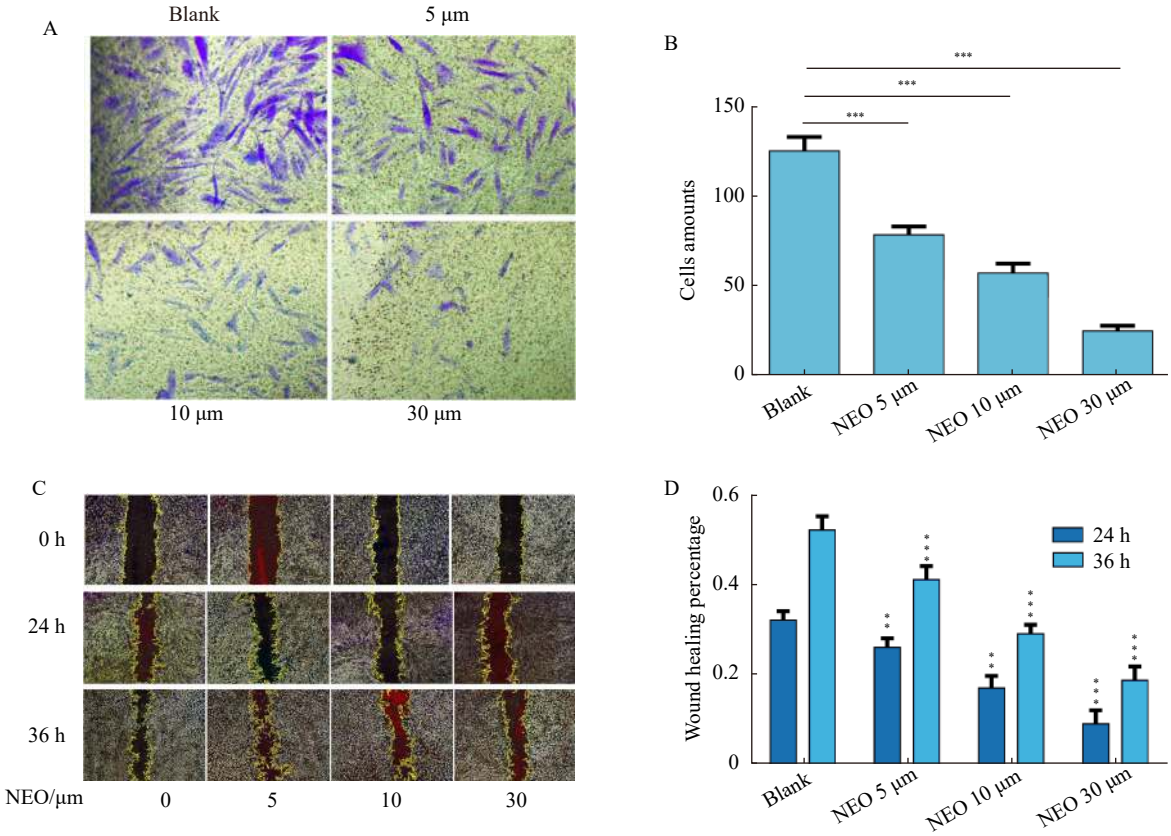

Fig. 3 Inhibitory effect of NEO on the invasion and migration of RA-FLSs. (A, B) Invased cells were detected by counting the cells that migrated to the lower side of a transwell chamber (magnification × 100/200, bar = 100 μm). (C, D) Images showing the migration of RA-FLSs treated with different concentrations of NEO (5.0, 10.0, and 30.0 μmol·L^{-1}) 24 h and 36 h after scratching. Data are presented as a percentage of scratched area at time 0 h. Values are mean ± SD from ≥ three independent experiments. Statistical difference is represented by $^{***}P < 0.001$, $^{**}P < 0.01$, $^{*}P < 0.05$ *vs* the blank group

current study, natural products were focused, and a novel function of Neo was found, which suppressed tumour-like properties of RA-FLSs through inhibiting its inflammation, invasion, migration, and ROS production while inducing its apoptosis. Our results further revealed that Neo can alleviate RA which are greatly assoicated with the MAPK pathway.

During the pathogenesis of RA, pro-inflammatory cytokines and MMPs are produced and secreted after the activation of RA-FLSs, which has become two of the major factors for inflammation and joint destruction [24]. It is well known that pro-inflammatory cytokines such as IL-1β, IL-6 and TNF-α, play an important role in the inflammatory response of RA. Cartilage destruction and bone erosion are largely attributable to increased expression of MMPs secreted by RA-FLSs [25, 26]. Among the MMPs, MMP-3, MMP-9 and MMP-13 are reported to be involved in RA progression [27]. Previous experiments confirmed that RA-FLSs can be activated and the production of inflammatory cytokines can increase upon stimulation with 10 ng·mL^{-1} TNF-α [28]. Our study showed that Neo inhibited MMP-3, MMP-9 and MMP-13 production in TNF-α-stimulated RA-FLSs as well as secretion of IL-1β, IL-6 and IL-8 at the concentrations of 5−30 μmol·L^{-1}. Further experiments without exogenous TNF-α-stimulation showed that Neo still alleviated inflammation compared with the blank group. In addition, Neo u-pregulated the expression of OPG mRNA while down-regulated RANKL expression in RA-FLS cells, which suggested that Neo can alleviate bone damage and osteoporosis in RA. The MAPK signaling pathway, by which inflammatory stimulants contribute to its activation, includes ERK, p38 and JNK [29, 30]. Notably, p38 activation regulates the expression of pro-inflammatory cytokines [31]. Erk1/2 activation plays an important role in the macrophages of RA through regulating cytokine production *via* transcriptional and post-transcriptional mechanisms [32]. In this study, pretreatment of Neo blocked the phosphorylation of ERK, JNK and p38 MAPK. Therefore, the MAPK signaling pathway may be correlated with Neo's anti-inflammation properties.

Among all the reported mechanisms about synovium hyperplasia, inadequate apoptosis is the most basic, dominant, and generally accepted oppinion. Among all the reported molecules and receptors in the regulation of cell apoptosis, the MAPK signaling pathway is significantly involved, which plays a dominant role in cell proliferation and apoptosis [33, 34]. As a distal component of the MAPK pathway, ERK acts as a key regulator in the cascade of some kinases and activity of

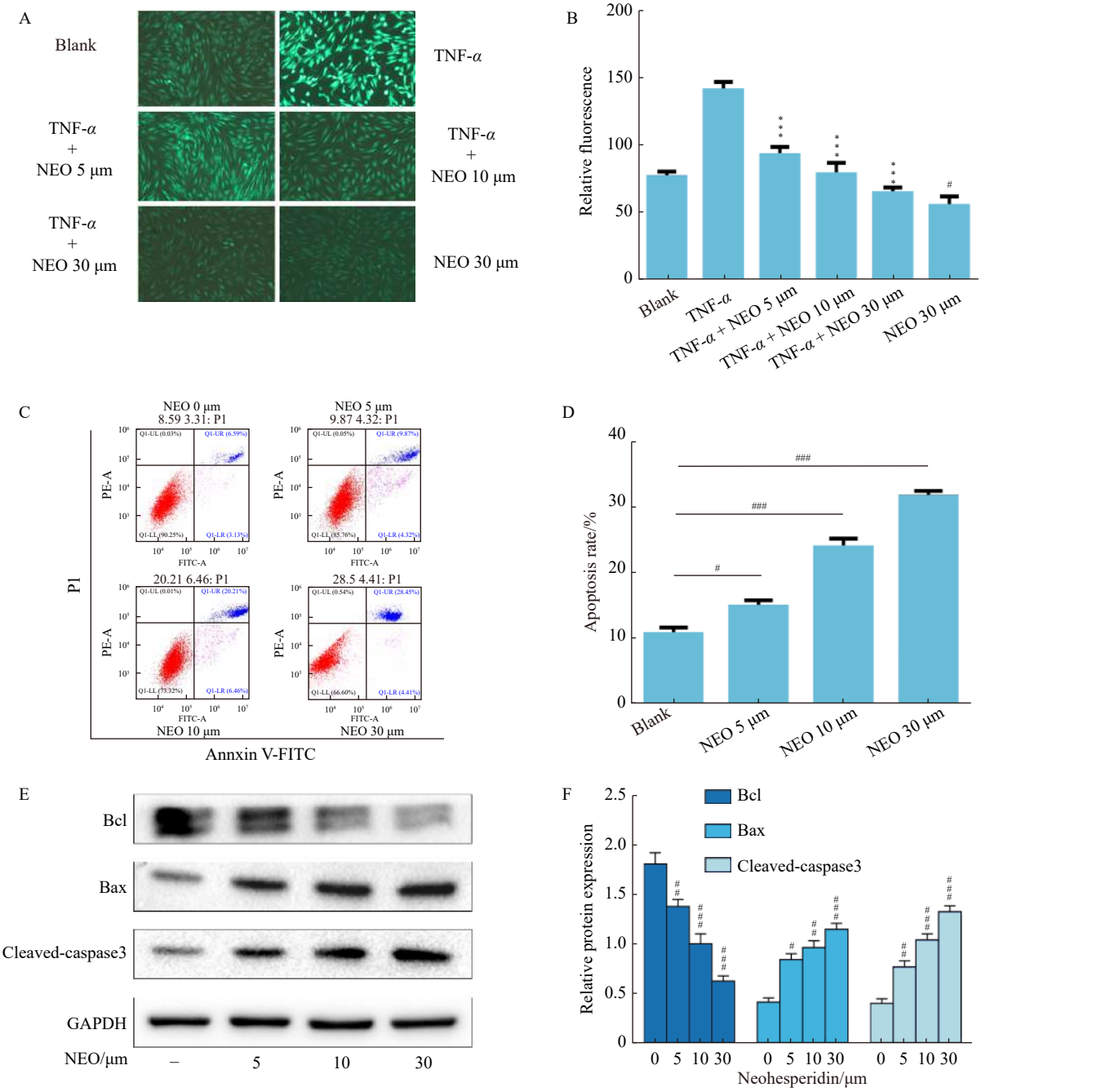

Fig. 4 Effect of NEO on intracellular ROS production and apoptosis of RA-FLSs. (A, B) Effect of NEO on intracellular ROS production after administration of TNF-*α* (10 ng·mL^{-1}) and different concentrations of NEO (5.0, 10.0, and 30.0 μmol·L^{-1}). The production of ROS was determined by immunofluorescence staining. (C, D) Cell apoptotic rate was detected by flow cytometry with Annexin V-FITC/PI double staining. (E, F) The expression of bcl-2, bax, and cleaved-caspase 3 was measured by Western blot. Values are mean ± SD from ≥ three independent experiments. Statistical difference is represented by $^{***}P < 0.001$, $^{**}P < 0.01$, $^{*}P < 0.05$ *vs* TNF-*α* sitimulated group. $^{###}P < 0.001$, $^{##}P < 0.01$, $^{#}P < 0.05$ *vs* the blank group

transcription factors. Therefore, ERK serves as a critical nuclear factor for cell apoptosis process [35, 36]. Once the phosphorylation of ERK1/2 is activated, it will result in elevated levels of Bcl-2 protein, thus influencing the proliferation and apoptosis of cells. Caspase-3 plays a very significant role in the execution phase of apoptosis. Bcl-2 family consists of anti-apoptotic proteins (Bcl-2) and pro-apoptotic proteins (Bax). The Bcl-2/Bax ratio as an index can determine the survival or death of cells following an apoptotic stimulus [37]. Our results indicated that the apoptosis rate in RA-FLS cells evidently increased after administration of Neo and the increased Bcl-2/Bax ratio was observed by Western blot. Moreover, Neo significantly suppressed the invasion and migration of RA-FLSs. The reason may be that Neo promotes the apoptosis of

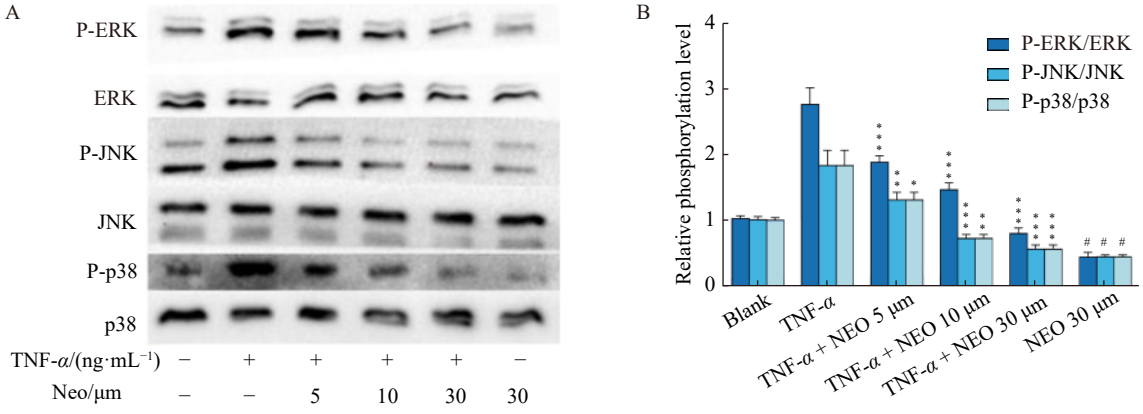

Fig. 5 Effect of NEO on TNF-*α* induced MAPK signaling pathway. (A) The expression of phosphorylated ERK (P-ERK), total ERK, phosphorylated JNK (P-JNK), total JNK, phosphorylated p38 (P-p38), and total p38, in RA-FLSs was tested by Western blot. (B) Gray level of Western blot. All data are expressed as mean ± SD (*n* = 3). Statistical difference is represented by $^{***}P < 0.001$, $^{**}P < 0.01$, $^{*}P < 0.05$ *vs* TNF-*α* sitimulated group. $^{###}P < 0.001$, $^{##}P < 0.01$, $^{#}P < 0.05$ *vs* the blank group

RA-FLSs and inhibits its migration and invasion, through down-regulating the activity of the MAPK signaling pathway.

Cells can produce cytokines such as superoxide radicals, hydrogen peroxide and hydroxyl radicals under the stress, which are generally called ROS. According to relevant studies, ROS production may result from the transfer of excess unpaired electrons in the oxidative respiratory chain to O_2 [38]. It is reported that a moderate increase in intracellular ROS level promotes cell proliferation, whereas excessive amounts of ROS trigger cell damage and induce cell apoptosis [39, 40]. Furthermore, previous studies indicated that ROS is particularly relevant to the dysfunction of mitochondrial in inflammatory diseases, especially in RA [41]. Another study demonstrated that RA-FLS cells display increased production of ROS, while ROS can mediate the migration of RA-FLSs and angiogenesis in RA [42]. Recently, it has been confirmed that the increased ROS production in RA-FLS cells facilitates mitochondrial dysfunction, thereby accelerating the pathogenesis of RA [43]. Our results supported the notion that TNF-*α* induces the production of ROS [44], while ROS accumulation is remarkably reversed after treatment of Neo in a concentration-dependent manner.

The functional link between ROS and MAPK still remains poorly understood. It was reported that H_2O_2 significantly increased the phosphorylation of p38 MAPK and Erk1/2, indicating the important role of ROS in mediating the MAPK signaling pathway [45]. Since Neo is capable of diminishing osteoclast resorption activity and inhibiting ROS production through inhibiting the MAPK signaling pathway [46], it is assumed that reduction of intracellular ROS level in RA-FLS cells may also be one of the reasons for inhibiting the MAPK signaling cascade.

Taken together, this study demonstrated that Neo exerts remarkable inhibitory effects against inflammation in RA-FLS cells, and exhibits anti-migration, anti-invasion,, anti-oxidative, and apoptosis-induced effects. It is demonstrated for the first time the regulatory effect of Neo on RA-FLSs potentially *via* the MAPK signaling pathway. These results may provide preliminary experimental evidence for supporting the treatment of Neo against RA.

References

[1] Widdifield J, Paterson JM, Bernatsky S, *et al*. The epidemiology of rheumatoid arthritis in Ontario, Canada [J]. *Arthritis Rheumatol*, 2014, **66**(4): 786-793.
[2] Mor A, Abramson SB, Pillinger MH. The fibroblast-like synovial cell in rheumatoid arthritis: a key player in inflammation and joint destruction [J]. *Clin Immunol*, 2005, **115**(2): 118-128.
[3] Coulombe P, Meloche S. Atypical mitogen-activated protein kinases: structure. regulation and functions [J]. *Biochim Biophys Acta*, 2007, **1773**(8): 1376-1387.
[4] Arthur JS, Ley SC. Mitogen-activated protein kinases in innate immunity [J]. *Nat Rev Immunol*, 2013, **13**(9): 679-692.
[5] Malemud CJ. Intracellular signaling pathways in rheumatoid arthritis [J]. *J Clin Cell Immunol*, 2013, **4**: 160.
[6] MacFarlane LA, Todd DJ. Kinase inhibitors: the next generation of therapies in the treatment of rheumatoid arthritis [J]. *Int J Rheum Dis*, 2014, **17**(4): 359-368.
[7] Meirinhos J, Silva BM, Valentao P, *et al*. Analysis and quantification of flavonoidic compounds from Portuguese olive (Olea europaea L.) leaf cultivars [J]. *Nat Prod Res*, 2005, **19**(2): 189-195.
[8] Roowi S, Crozier A. Flavonoids in tropical citrus species [J]. *J Agric Food Chem*, 2011, **59**(22): 12217-12225.
[9] Bitis L, Kultur S, Melikoglu G, *et al*. Flavonoids and anti-oxidant activity of Rosa agrestis leaves [J]. *Nat Prod Res*, 2010, **24**(6): 580-590.
[10] Vedpal, Jayaram U, Wadhwani A, *et al*. Isolation and characterization of flavonoids from the roots of medicinal plant *Tadehagi triquetrum* (L.) H.Ohashi [J]. *Nat Prod Res*, 2019, **34**(13): 1913-1918.
[11] Lale A, Herbert JM, Augereau JM, *et al*. Ability of different flavonoids to inhibit the procoagulant activity of adherent human monocytes [J]. *J Nat Prod*, 1996, **59**(3): 273-276.
[12] Shanmugam K, Holmquist L, Steele M, *et al*. Plant-derived polyphenols attenuate lipopolysaccharide-induced nitric oxide and tumour necrosis factor production in murine microglia and macrophages [J]. *Mol Nutr Food Res*, 2008, **52**(4): 427-438.
[13] Guo C, Zhang H, Guan X, *et al*. The anti-aging potential of neohesperidin and its synergistic effects with other citrus flavonoids in extending chronological lifespan of saccharomyces cerevisiae BY4742 [J]. *Molecules (Basel, Switzerland)*, 2019, **24**(22): 4093.
[14] Bellocco E, Barreca D, Laganà G, *et al*. Influence of L-rhamnosyl-D-glucosyl derivatives on properties and biological interac-

tion of flavonoids [J]. *Mol cell biochem*, 2009, **321**(1-2): 165-171.
[15] Patil JR, Chidambara Murthy KN, Jayaprakasha GK, *et al*. Bioactive compounds from Mexican lime (*Citrus aurantifolia*) juice induce apoptosis in human pancreatic cells [J]. *J Agr Food Chem*, 2009, **57**(22): 10933-10942.
[16] Wang SY, Sun ZL, Liu T, *et al*. Flavonoids from *Sophora moorcroftiana* and their synergistic antibacterial effects on MRSA [J]. *Phytother Res*, 2014, **28**(7): 1071-1076.
[17] Shi Q, Song X, Fu J,*et al* . Artificial sweetener neohesperidin dihydrochalcone showed anti-oxidative, anti-inflammatory and anti-apoptosis effects against paraquat-induced liver injury in mice [J]. *Int Immunopharmacol*, 2015, **29**(2): 722-729.
[18] Dhillon AS, Hagan S, Rath O, *et al*. MAP kinase signalling pathways in cancer [J]. *Oncogene*, 2007, **26**(22): 3279-3290.
[19] Gong Y, Dong R, Gao X, *et al*. Neohesperidin prevents colorectal tumorigenesis by altering the gut microbiota [J]. *Pharmacol Res*, 2019, **148**: 104460.
[20] Ugocsai K, Varga A, Molnár P, *et al*. Effects of selected flavonoids and carotenoids on drug accumulation and apoptosis induction in multidrug-resistant colon cancer cells expressing MDR1/LRP [J]. *In Vivo*, 2005, **19**(2): 433-8.
[21] F. Xu, J. Zang, D. Chen, *et al*. Neohesperidin induces cellular apoptosis in human breast adenocarcinoma MDA-MB-231 cells via activating the Bcl-2/Bax-mediated signaling pathway [J]. *Nat Prod Commun*, 2012, **7**(11): 1475-8.
[22] F.C. Arnett, S.M. Edworthy, D.A. Bloch, *et al*. The American Rheumatism Association 1987 revised criteria for the classification of rheumatoid arthritis [J]. *Arthritis Rheum*, 1988, **31**(3): 315-24.
[23] B. Bartok, G.S. Firestein. Fibroblast-like synoviocytes: key effector cells in rheumatoid arthritis [J]. *Immunol Rev*, 2010, **233**(1): 233-55.
[24] K.M. Doody, N. Bottini, G.S. Firestein. Epigenetic alterations in rheumatoid arthritis fibroblast-like synoviocytes [J]. *Epigenomics*, 2017, **9**(4): 479-492.
[25] Y. Araki, T. Mimura. Matrix Metalloproteinase Gene Activation Resulting from Disordred Epigenetic Mechanisms in Rheumatoid Arthritis [J]. *Int J Mol Sci*, 2017, **18**(5).
[26] Y. Itoh. Metalloproteinases in Rheumatoid Arthritis: Potential Therapeutic Targets to Improve Current Therapies [J]. *Prog Mol Biol Transl Sci*, 2017, **148**: 327-338.
[27] J. Withrow, C. Murphy, Y. Liu, *et al*. Extracellular vesicles in the pathogenesis of rheumatoid arthritis and osteoarthritis [J]. *Arthritis Res Ther*, 2016, **18**(1): 286.
[28] H. Du, X. Zhang, Y. Zeng, *et al*. A Novel Phytochemical, DIM, Inhibits Proliferation, Migration, Invasion and TNF-α Induced Inflammatory Cytokine Production of Synovial Fibroblasts From Rheumatoid Arthritis Patients by Targeting MAPK and AKT/mTOR Signal Pathway [J]. *Front Immunol*, 2019, **10**: 1620.
[29] J.D. O'Neil, A.J. Ammit, A.R. Clark. MAPK p38 regulates inflammatory gene expression via tristetraprolin: Doing good by stealth [J]. *Int J Biochem Cell Biol*, 2018, **94**: 6-9.
[30] T. Shimo, S. Matsumura, S. Ibaragi, *et al*. Specific inhibitor of MEK-mediated cross-talk between ERK and p38 MAPK during differentiation of human osteosarcoma cells [J]. *J Cell Commun Signal*, 2007, **1**(2): 103-11.
[31] F.M. Meier, I.B. McInnes. Small-molecule therapeutics in rheumatoid arthritis: scientific rationale, efficacy and safety [J]. *Best Pract Res Clin Rheumatol*, 2014, **28**(4): 605-24.
[32] Y.F. Chuang, H.Y. Yang, T.L. Ko, *et al*. Valproic acid suppresses lipopolysaccharide-induced cyclooxygenase-2 expression via MKP-1 in murine brain microvascular endothelial cells [J]. *Biochem Pharmacol*, 2014, **88**(3): 372-83.
[33] Y. Hu, L. Yang, Y. Yang, *et al*. Oncogenic role of mortalin contributes to ovarian tumorigenesis by activating the MAPK-ERK pathway [J]. *J Cell Mol Med*, 2016, **20**(11): 2111-2121.
[34] P. Zhao, W. Ma, Z. Hu, *et al*. Filamin A (FLNA) modulates chemosensitivity to docetaxel in triple-negative breast cancer through the MAPK/ERK pathway [J]. *Tumour Biol*, 2016, **37**(4): 5107-15.
[35] C.C. Reyes-Gibby, J. Wang, M.R. Silvas, *et al*. MAPK1/ERK2 as novel target genes for pain in head and neck cancer patients [J]. *BMC Genet*, 2016, **17**: 40.
[36] Y. Wang, C. Gao, Y. Zhang, *et al*. Visfatin stimulates endometrial cancer cell proliferation via activation of PI3K/Akt and MAPK/ERK1/2 signalling pathways [J]. *Gynecol Oncol*, 2016, **143**(1): 168-178.
[37] Z.N. Oltvai, C.L. Milliman, S.J. Korsmeyer. Bcl-2 heterodimerizes in vivo with a conserved homolog, Bax, that accelerates programmed cell death [J]. *Cell*, 1993, **74**(4): 609-19.
[38] S. Kovac, P.R. Angelova, K.M. Holmström, *et al*. Nrf2 regulates ROS production by mitochondria and NADPH oxidase [J]. *Biochim Biophys Acta*, 2015, **1850**(4): 794-801.
[39] M.H. Raza, S. Siraj, A. Arshad, *et al*. ROS-modulated therapeutic approaches in cancer treatment [J]. *J Cancer Res Clin Oncol*, 2017, **143**(9): 1789-1809.
[40] R. Wang, L. Ma, D. Weng, *et al*. Gallic acid induces apoptosis and enhances the anticancer effects of cisplatin in human small cell lung cancer H446 cell line via the ROS-dependent mitochondrial apoptotic pathway [J]. *Oncol Rep*, 2016, **35**(5): 3075-83.
[41] J.P. Sharman, J. Chmielecki, D. Morosini, *et al*. Vemurafenib response in 2 patients with posttransplant refractory BRAF V600E-mutated multiple myeloma. Clinical lymphoma [J]. *Clin Lymphoma Myeloma Leuk*, 2014, **14**(5): e161-3.
[42] Y. Zhou, Q. Zhang, O. Stephens, *et al*. Prediction of cytogenetic abnormalities with gene expression profiles [J]. *Blood*, 2012, **119**(21): e148-50.
[43] M. Al-Azab, E. Qaed, X. Ouyang, *et al*. TL1A/TNFR2-mediated mitochondrial dysfunction of fibroblast-like synoviocytes increases inflammatory response in patients with rheumatoid arthritis via reactive oxygen species generation [J]. *FEBS J*, 2020, **287**(14): 3088-3104.
[44] M. Bonora, E. De Marchi, S. Patergnani, *et al*. Tumor necrosis factor-α impairs oligodendroglial differentiation through a mitochondria-dependent process [J]. *Cell Death Differ*, 2014, **21**(8): 1198-208.
[45] D.Y. Rhyu, Y. Yang, H. Ha, *et al*. Role of reactive oxygen species in TGF-beta1-induced mitogen-activated protein kinase activation and epithelial-mesenchymal transition in renal tubular epithelial cells [J]. *J Am Soc Nephrol*, 2005, **16**(3): 667-75.
[46] Z. Tan, J. Cheng, Q. Liu, *et al*. Neohesperidin suppresses osteoclast differentiation, bone resorption and ovariectomised-induced osteoporosis in mice [J]. *Mol Cell Endocrinol*, 2017, **439**: 369-378.

Cite this article as: WANG Xiao-He, DAI Ce, WANG Jun, LIU Rui, LI Lei, YIN Zong-Sheng. Therapeutic effect of neohesperidin on TNF-α-stimulated human rheumatoid arthritis fibroblast-like synoviocytes [J]. *Chin J Nat Med*, 2021, **19**(10): 741-749.